SciMedCentral

JSM Nanotechnology & Nanomedicine

Research Article

Antimicrobial Activity of ZnO Nanoparticles against Pathogenic Bacteria and Fungi

Govinda R Navale[1], Thripuranthaka M[2], Dattatray J Late[2,3]* and Sandip S Shinde[1,3]*

[1]*Division of Organic Chemistry, National Chemical Laboratory (CSIR-NCL), Pune, India*

[2]*Physical and Materials Chemistry Division, National Chemical Laboratory (CSIR-NCL), Pune, India*

[3]*Academy of Scientific and Innovative Research, Anusandhan Bhawan, New Delhi, India*

Corresponding authors

Sandip S Shinde, Division of Organic Chemistry, CSIR-National Chemical Laboratory (CSIR-NCL), Pune, India, E-mail: ss.shinde@ncl.res.in

Dattatray J Late, Physical and Materials Chemistry Division, CSIR-National Chemical Laboratory (CSIR-NCL), Pune, India, E-mail: dj.late@ncl.res.in

Submitted: 05 December 2014

Accepted: 26 February 2015

Published: 02 March 2015

Keywords

- Nanoparticles
- Zinc oxide
- Antibacterial
- Antifungal
- Reactive oxygen species

Abstract

Antimicrobial growth inhibition and mechanistic activities of synthesized Zinc oxide nanoparticles (ZnO NPs) were investigated in this study. Nanoparticle size 20-25 nm and concentrations of 0, 20, 40, 60, 80 and 100 µg/mL were used against pathogenic bacteria *Staphylococcus aureus* (Gram positive) and *Salmonella typhimurium* (Gram negative) and also first time against two plant fungi *Aspergillus* strain of *flavus* and *fumigatus*. The growth analysis data indicated that the ZnO NPs have significant bactericidal effect on both the bacteria. The quantity of dried fungal biomass was negligible when the fungal culture was grown in presence of 100 µg/mL NPs. These microbial analyses data indicates that the ZnO NPs (size ~20-25 nm) have shown potential activity against these tested bacteria and fungi. Further examine the antimicrobial mechanisms of the ZnO NPs by UV photocatlytic and GSH oxidation methods, which suggested that ZnO NPs could produce reactive oxygen species, and also the oxidation capacity of NPs towards the γ-L-Glutamyl-L-cysteinyl-glycine (GSH) oxidation stress, were responsible for antimicrobial behaviour of ZnO NPs.

INTRODUCTION

Metal oxide nanoparticles and composite materials are widely applied in the field of research and development and diverse applications in industries including surface coatings, optoelectronics, bioengineering, biodignostics, and agriculture [1,2]. Their intrinsic properties are mainly determined by size, shape, composition, crystallinity and morphology. Highly ionic zinc oxide nanoparticles are unique in that they can be produced with high surface area, unusual crystal structures and size. The main advantages of using ZnO nanoparticles have excellent stability or long shelf life with organic antimicrobial agents [2]. In particular, the vigorous antimicrobial properties of nanoscale ZnO particles have been the focus of industrial applications in biocides coating in water treatment, paints and cosmetic products [3]. The scope of ZnO nanoparticles has been a keen area of interest for biologist due to their distinguished antimicrobial and distinct activity which has opened new frontiers to biological sciences [4]. Especially in its nanoscale form has a strong toxicity towards a wide range of micro-organisms including bacteria [5], fungi [6], fish [7], algae [8] and plants [9]. To find out the antibacterial activity of nanoparticles the pathogenic bacteria, such as *Escherichia coli* and *Staphylococcus aureus* strains are being well know for initial investigation [10]. Growth of fungal pathogens in plants is the main cause of considerable economic loss during postharvest handling of grains and fruits. The fungal growth is difficult to control by organic substrate because fungi have developed resistance to many conventional fungicides such as benzimidazoles and dicarboximides [11]. Fungus *Aspergillus* species infection to plant will reduce the 20-30% total crop yield; this crop loss can be control by various metal nanoparticles because it has strong antifungal effect against specific fungi [12]. Infections of Aspergillus species have been identified and they are of major concern to the agriculture production losses.

We recently studied the ZnO NPs has different optical, field emission properties and applications in the field of nanotechnology [13-15]. Our continuous interest in ZnO nanoparticles, herein the structure and composition of freshly synthesized ZnO NPs 20-25 nm in size and spherical and hexagonal shaped were examined and evaluate influences against common pathogenic bacteria *S. aureus* (Gram-positive) and first time with *S. typhimurium* (Gram-negative) and two new agricultural important pathogenic fungus from *Aspergillus* family. As per our literature survey, this is first time to investigate the effect of ZnO nanoparticles with bacteria *S. typhimurium*, and fungus *A. flavus* and *A. fumigatus.* Also figure

out the possible mechanism of antimicrobial effects by photo catalytic and GSH-Oxidation study.

MATERIALS AND METHODS

Synthesis of ZnO Nanoparticles

To prepare of ZnO nanoparticles, precipitation method was applied according to modified procedure reported by Sourabh D *et al.,* [16], The ZnO nanoparticles were successfully synthesised using zinc acetate di-hydrate (Zn $(OAc)_2$. $2H_2O$, 0.3M) and xylene (C_8H_{10}) in 100 mL of methanol (MeOH) under constant stirring. In a typical experiment: The zinc acetate dihydrate (Zn $(OAc)_2$. $2H_2O$) and xylene (C_8H_{10}) were diluted in equal (1:1) ratio in MeOH and stirred the solution for 30 min to complete dissolution of acetate salt. The pH of this solution was measured and it was reached around 6.7 to 6.8. The solution was transferred to the three necked refluxing flask and was refluxed at, 65^0C for 6 h and then air cooled at room temperature. With rise in refluxing temperature, the transparent solution was changed in to white suspension and white precipitate was achieved in 6 h. No precipitate was observed before 6 h. The obtained precipitate has been washed several times by centrifuging it at 5000 rpm for 10 min with methanol, ethanol and acetone to remove the ionic impurities and dried it by keeping it in hot air oven at 100^0C for 24 h in a glass petridish. The white powder sample then further crushed with a mortar and pestle to obtain fine nano sized ZnO NPs.

Characterization

The crystal structure, size, and shape of the synthesized ZnO nanoparticles were investigated using powder X-ray diffraction (XRD) and transmission electron microscopies (TEM). ZnO nanoparticles were suspended in de-ionized water and ultrasonicated for about 10 min and a clear dispersion of which is drop casted on to a carbon film coated Cu grids for collecting high resolution transmission electron microscopy images (HRTEM), For recording the X-ray diffraction (XRD) pattern ZnO nanoparticles were coated into a thin film on a cleaned glass substrate and for recording the Raman spectrum the sample was prepared in the similar way as for XRD.

TEM images were collected using FEI TECNAI TF-30 (FEG) instrument. XRD patterns were collected between the angles 20 to 80 degrees at a scan rate of 1 degree per minute using the XPERT PRO diffractometer. Raman spectra were collected with Lab RAM HR with a laser source of 632.8 nm at a power of ~200 μW at the sample in the back scattering geometry. UV-Vis spectrum was collected from JASCO v570 instrument. UV- Vis absorption spectrum of the ZnO nanoparticles was recorded in the solution form.

Microbial strains and culture conditions

In this experiment, four representative pathogenic microorganisms were selected, including two bacterial pathogens (*Staphylococcus aureus* ATCC29737/NCIM-2901 and *Salmonella typhimurium* ATCC 23564/NCIM 2501) and two fungal plant pathogens (*Aspergillus flavus* NCIM-524 and *Aspergillus fumigatus* NCIM-902). The four microbes were all taken from National Collection of Industrial Microorganisms (NCIM) Pune, India. *S. aureus* and *S. typhimurium* were grown in LB (Luria-Bertani, Hi-Media, India) broth medium in a humidified incubator at 37ºC with constant agitation overnight whereas *A. flavus* and *A. fumigatus* were sub cultured and isolated on sabouraud dextrose agar and broth (Himedia Mumbai, India). Cultures were inoculated from isolated colony into Sabouraud Dextrose Broth and grown aerobically at 30°C.

ANTIBACTERIAL ACTIVITY OF ZnO NANOPARTICLES

Minimal Inhibitory Concentration (MIC) Determination

To investigate the minimum inhibitory concentration (MIC) of ZnO NPs against both *S. aureus* and *S. typhimurium* were determined by a method recommended in NCCLS [18]. Briefly, the sterile tubes were incubated aerobically at 37°C for 24 h with 180 rpm, which contained 5 mL Muller-Hinton (MH) broth (Hi-media-India) with approximate 5×10^7 CFU/mL of Gram-positive *S. aureus* and Gram-negative *S. typhimurium* cells with various concentration of ZnO nanoparticles (20 μg/mL, 40 μg/mL, 60 μg/mL, 80 μg/mL, 100 μg/mL). The concentration of tube without visible growth of both the bacterial cells was the MIC and which is measure by taking optical density at 600 nm by using UV-spectrophotometer (JASCO-530) after 24 h incubation. All the measures were triplicate.

Bacterial cell growth and Viability Testing

To examine the bacterial growth rate or the bacterial growth behavior in the presence of 20-25 nm sized ZnO nanoparticles *S. aureus* and *S. typhimurium*, both the bacterial cultures were harvested in the mid exponential growth phase and the cells were collected by centrifugation at 6000 rpm for 10 min. Subsequently, the bacterial bread was washed three times with saline water to wipe off the medium constituents and other chemical macromolecules. Finally, the cells were re-suspended in saline water and the suspensions were progressively diluted to a desired concentration of 10^7 to 10^8 CFU/mL. 200μL of the diluted cell suspensions was mixed with 20 μL of five different concentrations of ZnO NPs (20 μg/mL, 40 μg/mL, 60 μg/mL, 80 μg/mL, 100 μg/mL) prepared in deionized water) along with a control and incubated at 37ºC for 2 h with gentle shaking. A control sample contained 200 μL of the cell suspensions and 20 mL of saline. The mixture was then transferred to 5 mL tubes, each containing 2 mL MH medium (Muller Hinton broth ,Hi-media, India) and the tubes were incubated on a rotary shaker at 150 rpm and 37ºC. The value of optical density (OD) at a wavelength of 600 nm was measured on a UV-VIS spectrometer every 2 h. Bacterial growth curves were created by plotting OD values versus time. All treatments were prepared in triplicate.

For antibacterial activity (Viability) test, the bacteria (10^7 to 10^8 CFU/mL) were incubated with different concentrations of ZnO for 4 h, and then 20μL of a serial 10^6-fold dilution of each bacterial suspension in sterile deionized water was spread onto LB plates and let to grow for 24 at 37ºC. Colonies were counted and the cell mortality (% of the control) was expressed as the percentage of [(counts of the control-counts of the treated samples)/counts of the control] X 100. All treatments were

individually repeated at least three times.

Antifungal Activity

The antifungal activity of ZnO NPs towards, *A. flavus* and *A. fumigatus* was studied by using modified Broth dilution Method, recommended in NCCLS 2002 protocol [19]. Sterile tubes containing 5mL Sabouraud Dextrose broth (Himedia Mumbai, India) inoculated with *A. flavus* or *A. fumigatus* were incubated along with different concentrations of ZnO nanoparticles at 37°C and 225 rpm for 24 to 72 h. The OD was measured after every 24 h at 410 nm. The experiment was conducted in triplicate.

In order to measure the fungal biomass/dry weight we applied similar method as previously reported [20]. After 7 days incubated fungal samples were then filtered through Whatman No.1 filter paper. Then the paper with fungal filtrate was dried at 50°C for 24 h in hot air oven and was used to determine the fungal biomass. The net wet of mycelia was determined by eliminating the weight of filter paper.

Detection of superoxide radical anions ($O_2^{\cdot-}$)

To find out the reactive oxygen species antibacterial paths, the possibility of superoxide radical ($O_2^{\cdot-}$) anion production was evaluated by measuring the absorption at 470 nm after the exposure of ZnO NPs to UV radiation for 2 h to 6 h, as ZnO NPs has a photo catalytic activity previously reported [21]. The 1 mg/mL ZnO disperse in DI water, After 10 min ultra-sonication, it was exposed to UV light ((365 nm, 66.2 mW/cm^2, Blak-Ray Longwave Ultraviolet Lamp B 100 AP) for different time interval. The produced superoxide radical was measured by taking out sample and then filtered it with whatmann filter paper. 250µL filtrate was taken and their absorbance at 470 nm was measured on a microplate spectrophotometer (Thermo Scientific Varioskan™ Flash Multimode Reader). TiO_2 NPs used as a positive control.

In vitro GSH oxidation and quantification

For the quantification of GSH oxidation was examined by the Ellmans assay [22]. The dispersion of the ZnO (250 µl of 20 µg/mL and 100 µg/mL NPs) in 50 mM bicarbonate buffer (pH 8.6) was added into 250 µL of GSH (γ-L-Glutamyl-L-cysteinyl-glycine Reduced 98%, Sigma Aldrich) (0.8 mM in the bicarbonate buffer) to initiate oxidation. The mixtures were covered with alumina foil to prevent illumination, and then placed in a shaker with a speed of 160 rpm at room temperature for incubation of 2-6 h. After incubation, 785 µL of 0.05 M Tris–HCl and 15 µL of DNTB (Ellman's reagent, 5, 50-dithio-bis-(2-nitrobenzoic acid), Sigma-Aldrich) were added into the mixtures to yield a yellow product. The ZnO NPs was removed from the mixtures by centrifuging it at 4000 RPM for 5 min. A 250 µL aliquot of supernatant from each sample was then placed in a 96-well plate. All tests were prepared in triplicate. Their absorbance at 412 nm was measured on a microplate spectrophotometer (Thermo Scientific Varioskan™ Flash Multimode Reader). GSH solution without ZnO Nps was used as a negative control. GSH (0.4 mM) oxidization by H_2O_2 (1 mM) was used as a positive control. The loss of GSH was calculated by the following formula: loss of GSH (%) = (absorbance of negative control -absorbance of sample)/ absorbance of negative control x 100.

RESULTS AND DISCUSSION

Characterization of ZnO NPs

The synthesized ZnO NPs were characterized based on data as shown in Figure 1. The TEM images of the ZnO NPs from which the average of nanoparticle were calculated to be ~20 nm with spherical and hexagonal shaped was observed (Figure 1a and 1b). Figure c of 1 shows the typical selected area of electron diffraction pattern (SAED) of the ZnO NPs which confirms the highly crystalline nature of ZnO NPs [23]. The Raman spectrum of ZnO NPs was excited with 632.8 nm laser source with a power of 200 µW recorded in the standard back scattering geometry (Figure 1e). From the spectrum we observed two significant peaks 436.5 cm^{-1} corresponding to the Raman active E_2 mode and the 607.9 cm^{-1}. These observed peaks consistent with the wurtzite structure of ZnO NPs reported earlier [24]. The powder XRD pattern of the ZnO NPs is shown in Figure f of 1. The typical peaks observed in the pattern correspond to the planes (100), (002), (101), (102), (110), (103), (112) and (201) and are in good agreement with the spherical and hexagonal wurtzite structure of bulk ZnO as confirmed by comparison with the JCPDS card (#36-1451). This powder XRD data indicate the ZnO NPs are in the wurtzite structure. The UV-Vis absorption spectra of the obtained ZnO NPs are in the range of 200 nm to 800 nm. We observe the a typical absorption peak at~ 310 nm as shown in Figure 1 (d), which corresponds to a band gap of 3.9 eV, was consistent to the previous report [25].

Antibacterial Activity

The minimal inhibitory concentration (MIC) of ZnO NPs towards the both the pathogenic bacteria Gram positive *S. aureus* and Gram negative *S. typhimurium* were 40 µg/mL, which were determined by taking absorbance at 600 nm after 24 h of incubation of bacterial cells. Chemically synthesized nanoparticles were unable to diffuse through agar medium. We observed the MIC value of ZnO NPs against *S. aureus* and *S. typhimurium* was almost similar (40 µg/mL). The minimum bactericidal concentration (MBC), after plating of 100 µg/mL ZnO NPs treated bacterial medium it showed the no growth on the LB plates (<5 colonies). In bacterial growth curve experiment, ZnO NPs had slightly more activity against *S. aureus* than *S. typhimurium* till 8 h. Concentration of 60 µg/mL ZnO NPs showed the bacteriostatic affect against both the pathogens but 80 µg/mL ZnO NPs had shown the completely inhibitory effect against *S. typhimurium* (Figure 2). In case of *S. aureus,* 80 µg/mL and 100 µg/mL ZnO showed the completely antibacterial activity, ZnO NPs retards the growth of both the pathogens when they are present in the bacterial suspension. Since the gram positive bacteria more susceptible towards metal nanoparticles as previously reported [5], surprisingly we found this ZnO NPs has shown quite similar activity against both bacteria.

In the viability test, the viability of the *S. aureus* and *S. typhimurium* decreases with increase in the concentration of ZnO NPs (Figure 3). After 4 h of incubation nearly 50 ± 1.9 % of *S. aureus* cells lost their viability in the concentration at 60 and 100

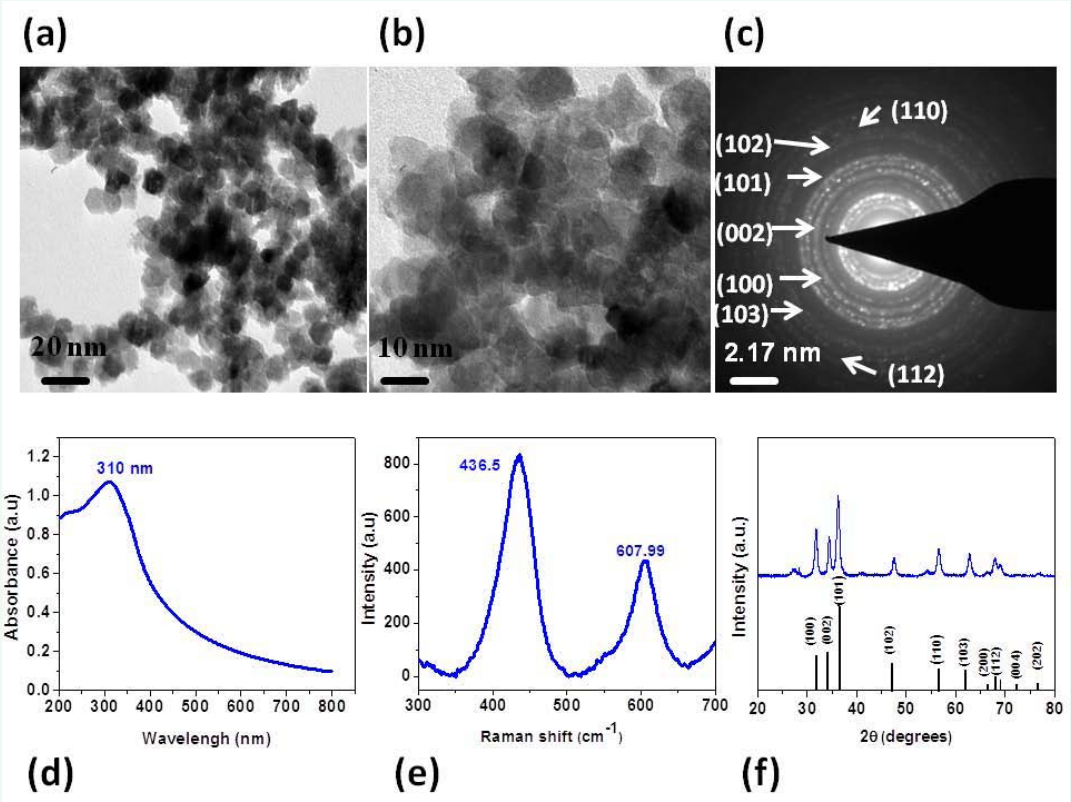

Figure 1 Synthesized ZnO nanoparticle (a, b) TEM images, (c) SAED pattern, (d) UV-Visible spectrum, (e) Raman spectrum, and (f) XRD pattern and also corresponding JCPDS Card No 36-1451 for hexagonal Wurtzite-typed ZnO were shown in inset down.

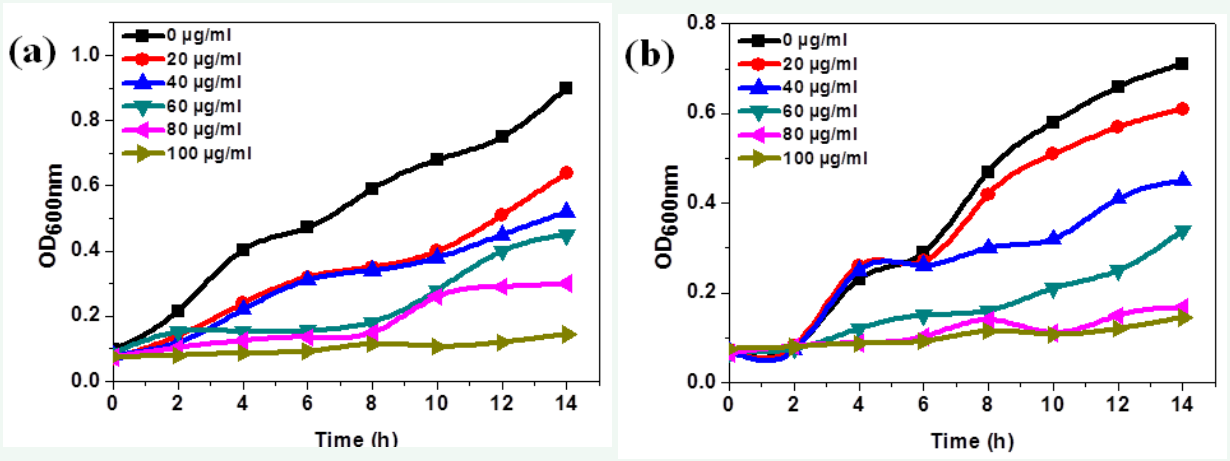

Figure 2 The effect of ZnO NPs on the growth of *S. aureus* (a) and *S. typhimurium* (b) culture in MH broth containing various concentrations of ZnO NPs (0 µg/mL control, 20 µg/mL, 40 µg/mL, 60 µg/mL, 80 µg/mL, 100 µg/mL) was grown at 37ºC with shaking at 225 rpm. The growth curve was determined by measuring the OD_{600nm} of the sample versus time (h).

µg/mL of NPs, as result the almost 95 ± 1.5 % of lost viability as compare to the control (Figure 4 compare a-c). On the other hand after 4 h of incubation *S. typhimurium* lost 75 ± 1.8 % viability in presence of 80µg/mL and more than 90 ± 1.4 % in 100 µg/mL ZnO NPs concentration compared to the control (Figure 4 compare d-f). This excellent antibacterial activity of ZnO NPs is due to the high surface area of smaller in size nanoparticles and ROS production.

Antifungal Activity

As per the our literature survey there is few studies over the antifungal activity of ZnO NPs. Fungi static activity of ZnO nanoparticles were investigated by the broth dilution method according to protocol in NCCLS [19]. Antifungal activity of the ZnO NPs against two major plant and animal pathogenic fungi *viz*. *A. fumigatus* and *A. flavus* is first time reported in this study.

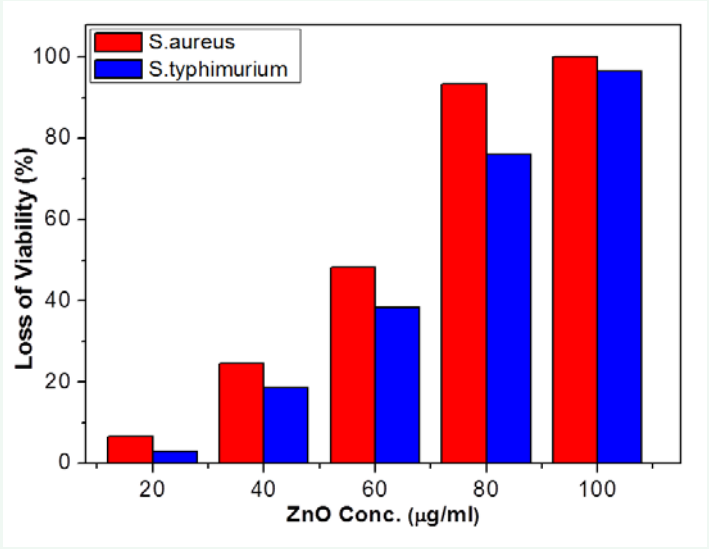

Figure 3 The viability of *S.aureus* and *S. typhimurium* cells after incubating with ZnO suspensions (20µg/mL, 40µg/mL, 60µg/mL, 80µg/mL and 100µg/mL) for 4 h with 220 rpm shaking speed at 37°C. Loss of viability was calculated by the following formula: loss of viability % = {(counts of control – counts of samples after incubation with suspensions)/counts of control}X 100.

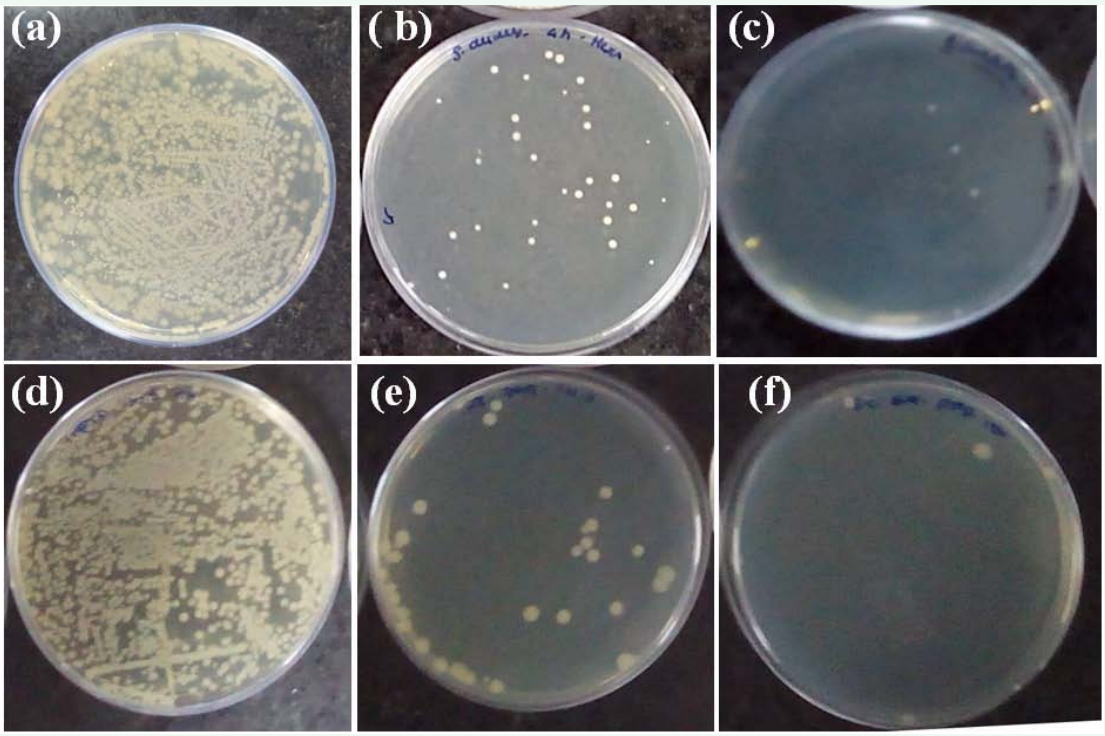

Figure 4 The viability of bacterial cells with ZnO NPs after incubating for 4 h with 220 rpm shaking speed at 37°C. *S.aureus* with a) control 0 µg/mL, b) 80 µg/mL and c) 100 µg/mL; *S. typhimurium* cells with d) control 0 µg/mL, e) 80 µg/mL and f) 100 µg/mL concentration.

From the concentration of 20 µg/mL ZnO NPs started to elicit inhibitory activity against plant pathogenic fungi *A. flavus* and *A. fumigatus* (graph not shown). However after 3 days of incubation by comparing optical density at 410 nm, 60 µg/mL and 80 µg/mL ZnO NPs showed the excellent activity against *A. fumigatus* and *A. flavus* respectively. After 7 days of incubation of both the fungi with different concentration of ZnO NPs, the fungal biomass was significantly decreased as the concentration of ZnO NPs was increases greater than 40 µg/mL. Figure 5, clearly reveals that the up to 75% of fungal biomass was reduced in presence of ZnO NPs 80 µg/mL concentrations. After a 7 days of incubation, the all the fungal biomasses were collected on filter paper, which showed significant antifungal role of ZnO NPs (Figure 6). However, the both fungi treated with ZnO NPs showed nearly similar

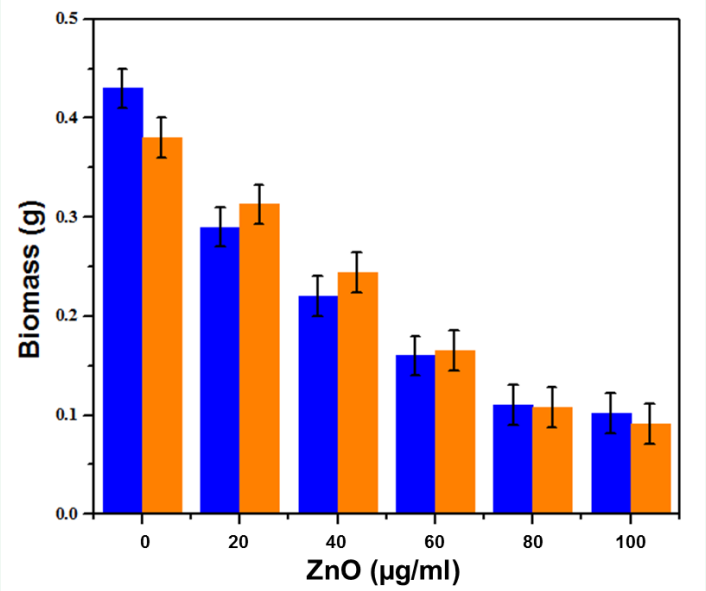

Figure 5 Effect of different concentrations of ZnO NPs on direct biomass of *A. flavus* (blue) and *A. fumigatus* (orange) after 7 day of incubation (values ± 0.02 g).

Figure 6 Fungal biomass harvested on filter paper treated with ZnO NPs, *A. flavus* with (a) control, (b) 80µg/mL. *A. fumigatus* with (c) control, (d) 80µg/mL concentration.

inhibitory effects but *A. fumigatus* slightly was more susceptible as compared to *A. flavus* (compare Figure 5 and 6). These results indicated that as the concentration of ZnO increases, the dry biomass of fungi decreases, up to the concentration 100 µg/mL. The analysis of the data can be applied to the analysis of protein quantity from total fungal mass [20].

These results clearly demonstrate that the zinc oxide could be the good antifungal agent against pathogenic fungi that can help to avoid crop infection of not only *A. flavus* and *A. fumigatus* but also the other species of *Aspergillus* as well as other similar fungi.

Antimicrobial Mechanism

Previous studies on the antibacterial Behavior of Zinc NPs have shown that the morphology and oxidative stress play important roles in the antibacterial activity [16,17]. Due to the quite similar nano sized structure of our ZnO NPs to other oxide nano particles, we examine oxidative stress in presence of NPs in order to explore how ZnO NPs kills the microorganisms including bacteria and fungi. To demonstrate the antibacterial mechanism of the ZnO NPs, we applied two methods, photo catalytic and GSH oxidation protocol to measure the superoxide anion production. Normally, oxidative stress may come from nanomaterials itself and other one it may came through disturbing microbial process or oxidizing a vital cellular structure or components without ROS production, i.e ROS independent oxidative stress [26,27].

TiO_2 radiated with UV light was used as a positive control to validate our tests and along ZnO NPs (without radiating with UV light) as a negative control. As shown in Figure 7, we found that ZnO NPs has the property to generate ROS in the presence of UV light; it could show significant antimicrobial activity in the presence of UV light because of ROS generation in the medium. After the 2, 4 and 6h incubation in UV radiation ZnO NPs have shown ascending level of absorbance that confirmed the ZnO NPs could be produce super oxide anion.

We further carried *in vitro* GSH oxidation protocol to figure out the second possible mechanism, as GSH is an antioxidant to bacteria and fungi of plants, to examine the possibility of ROS-

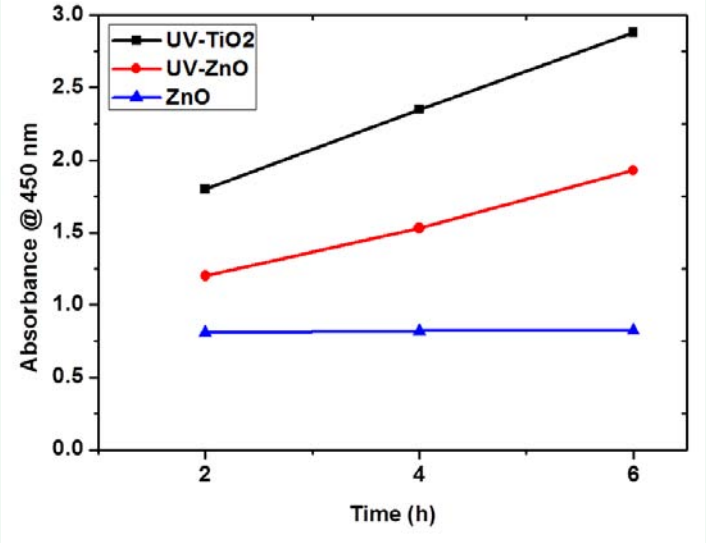

Figure 7 Time dependent photo catalytic activity of ZnO NPs. ZnO NPs was incubated in the presence of UV radiation, 2h, 4 h and 6 h. TiO_2 was used as a positive control and ZnO Nps without UV-radiation was used as a negative control.

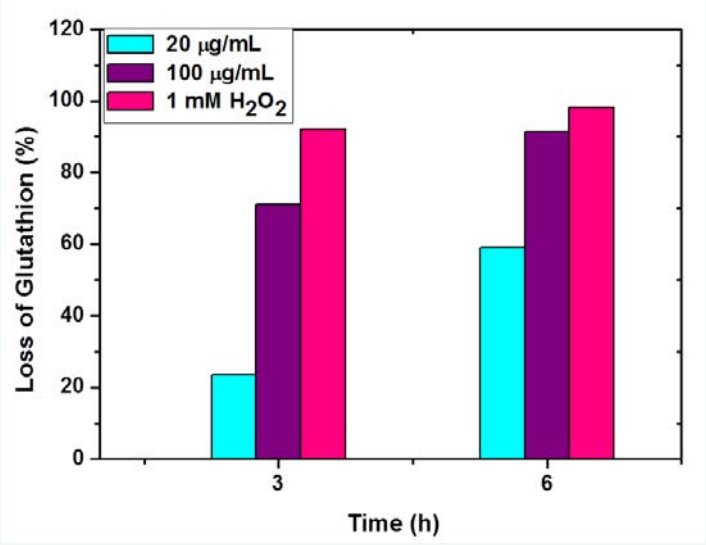

Figure 8 Time and concentration dependent GSH oxidation of ZnO Nps. 20 µg/mL and 100 µg/mL ZnO NPs were incubated with GSH (0.4 mM) for 3 h and 6 h. H_2O_2 (1 mM) was used as a positive control.

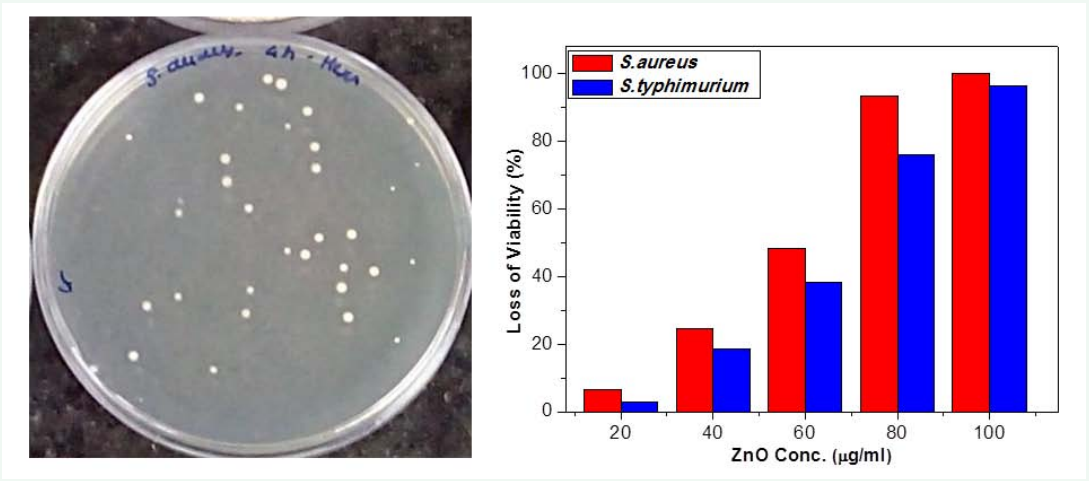

TOC

independent oxidative stress because this path play a significant role in the antimicrobial as well as toxic activity of nanoparticles [28,29]. Mechanism of GSH is a tripeptide with thiol groups (–SH) can be oxidized to form disulphide (–S–S–), converting GSH to glutathione disulphide. In bacteria GSH found of a concentration in the range from 0.1 to 10.0 mM preventing damages to cellular components. the employed the assay content, bicarbonate buffer (50.0 mM at pH 8.6) was used as negative control and H_2O_2 (1.0 mM) without ZnO NPs was used as a positive control in GSH oxidation experiments. As shown in Figure 8, the ZnO NPs had a capacity to oxidise GSH. The oxidation capacity of the ZnO NPs toward GSH was above 91.5 ± 1.4 % and above 55.6 ± 1.5 % after the incubation of 6 h with 100 µg/mL and 20 µg/mL ZnO NPs concentrations. The oxidation capacity of the ZnO NPs toward GSH was examine by taking absorbance at 412 nm. This incubation time and concentration dependent oxidation capacity is well consistent with the antibacterial activity as observed in Figure 8. These experiments proved that the antimicrobial activity of ZnO nanoparticles is dependent on the size of the nanoparticles and is mainly due to the particulate ZnO as the release of free Zn^{2+} ions and Reactive Oxygen Species (ROS) from ZnO colloidal solution is low in the experiment, these results are consistent with earlier report of ZnO NPs with spherical shapes and 15-20 nm size [17]. We realize the potential applications of ZnO NPs in medical fields so, to get a better understanding of the antimicrobial toxicity mechanism, the possibility of superoxide anion induced by ROS production was evaluated by UV-mediated photo catalytic experiment, and *in vitro* GSH (g-L-glutamyl-L-cysteinylglycine) oxidation methods. Our study suggests that the ZnO NPs and their photo catalytic properties contribute greatly to their antimicrobial activity with membrane and oxidation stress.

CONCLUSION

In conclusion, the ZnO NPs sizes of 20-25 nm possess significant antibacterial properties against *S. aureus* and *S. typhimurium*. Our results suggested that the ZnO NPs have greater efficacy in inhibiting the growth of *S. aureus* compared to the *S. typhimurium* and it's inhibitory effects increases as the concentrations of ZnO NPs increased. The concluded MIC for *S. aureus* and *S. typhimurium* was 40 µg/mL, In case of both fungi the concentration of ZnO NPs 80 to 100 µg/mL were more enough to significantly control their growth, which was demonstrated by weighing the fungal biomass. The antimicrobial mechanisms of the ZnO NPs, suggested that oxidation capacity of NPs toward GSH oxidation stress were responsible for antimicrobial behaviour of ZnO NPs. The results of *S. typhimurium*, and fungi *A. flavus* and *A. fumigates* suggest that ZnO nanoparticles are not only useful as an effective fungicide in agricultural and food packaging applications but also to control the growth of pathogenic bacteria.

ACKNOWLEDGEMENTS

Authors, S.S.S. and D.J.L., would like to thank DST (Government of India) for the Ramanujan fellowship (Grant No. SR/S2/RJN-111/2012 and SR/S2/RJN-130/2012). The research was primarily supported by DST Fast Track scheme for Young scientist project is gratefully acknowledged (Grant No. SB/FT/CS-042/2013 and SB/FT/CS-116/2013), and NCL-MLP project grant 028626, and the partial support by INUP IITB project sponsored by DeitY, MCIT, Government of India. Thanks to Director CSIR-NCL for constant support and encouragement.

REFERENCES

1. Soosen SM, Bose L, George KC. Optical Properties of ZnO Nanoparticles. SB Academic Review. 2009; 57-65. b) Nathaniel LR, Chad AM. Nanostructures in Biodiagnostics Chem. 2005; 105: 1547-1562
2. Kolodziejczak-Radzimska A, Jesionowski T. Zinc Oxide-From Synthesis to Application. Materials. 2014; 7: 2833-2881.
3. Ravishankar RV, Jamuna BA. Nanoparticles and their potential application as antimicrobials. A Méndez-Vilas A, editor. Mysore: Formatex. 2011; 197-209.
4. Allahverdiyev AM, Kon KV, Abamor ES, Bagirova M, Rafailovich M. Coping with antibiotic resistance: combining nanoparticles with antibiotics and other antimicrobial agents. Expert Rev Anti Infect Ther. 2011; 9: 1035-1052.
5. a) Huang Z, Zheng X, Yan D, Yin G, Liao X, Kang Y, et al. Toxicological effect of ZnO nanoparticles based on bacteria. Langmuir. 2008; 24: 4140-4144. b) Abdelhay A, Carmen-Mihaela T, Christophe M, Cédric M, Hélène G, Ghouti M, Raphaël S. Physicochemical properties and cellular toxicity of (poly) aminoalkoxysilanes-functionalized ZnO

quantum dots. Nanotechnology. 2012; 23: 335101.

6. He L, Liu Y, Mustapha A, Lin M. Antifungal activity of zinc oxide nanoparticles against Botrytis cinerea and Penicillium expansum. Microbiol Res. 2011; 166: 207-215.

7. Lin S, Zhao Y, Xia T, Meng H, Ji Z, Liu R. High content screening in zebrafish speeds up hazard ranking of transition metal oxide nanoparticles. ACS Nano. 2011; 5: 7284-7295.

8. Wong SW, Leung PT, DjurisiÄ‡ AB, Leung KM. Toxicities of nano zinc oxide to five marine organisms: influences of aggregate size and ion solubility. Anal Bioanal Chem. 2010; 396: 609-618.

9. Lin D, Xing B. Root uptake and phytotoxicity of ZnO nanoparticles. Environ Sci Technol. 2008; 42: 5580-5585.

10. Brayner R, Ferrari-Iliou R, Brivois N, Djediat S, Benedetti MF, Fiévet F. Toxicological impact studies based on Escherichia coli bacteria in ultrafine ZnO nanoparticles colloidal medium. Nano Lett. 2006; 6: 866-870.

11. Elad Y, Yunis H, Katan T. Multiple fungicide resistance to benzimidazoles, dicarboximides and diethofencarb in field isolates of Botrytis cinerea in Israel. Plant Pathol. 1992; 41; 41-46.

12. Roy SC, Ghosh M, Mandal A, Chakravorty D, Pal M, Pradhan S, et al. Surface-modified sulfur nanoparticles: an effective antifungal agent against Aspergillus niger and Fusarium oxysporum. Appl. Microbiol. Biotechnol. 2011; 90: 733-743.

13. Singh J, Kumara P, Late DJ, Singh T, More MA, Joag DS, et al. Optical and field emission properties in different nanostructures of ZnO. Dig. J. Nanomater. Bios. 2012; 7: 525-536.

14. Ramgir NS, Mulla IS, Vijayamohanan K, Late DJ, Bhise AB, More MA, et al. Ultralow threshold field emission from a single multipod structure of ZnO. Appl. Phys. Lett. 2006; 88: 042107

15. Ramgir NS, Late DJ, Bhise AB, More MA, Mulla IS, Joag DS, et al. ZnO Multipods, Submicron Wires, and Spherical Structures and Their Unique Field Emission Behavior. J Phys Chem B 2006; 110: 18236-18242.

16. Sourabh D, Rizwan W, Farheen K, Yogendra KM, Javed M, Abdulaziz AA. Reactive Oxygen Species Mediated Bacterial Biofilm Inhibition via Zinc Oxide Nanoparticles and Their Statistical Determination. PLoS One. 2014; 9: 111289.

17. Krishna RR, Ranjit TK, Adhar CM. Size-Dependent Bacterial Growth Inhibition and Mechanism of Antibacterial Activity of Zinc Oxide Nanoparticles. Langmuir, 2011; 27: 4020-4028.

18. NCCLS. Method for dilution antimicrobial susceptibility tests for bacteria that grow aerobically. Approved standard; 5 th ed. document M7-A5; NCCLS 2000; Wayne.

19. NCCLS. Reference method for broth dilution antifungal susceptibility testing of conidial forming filamentous fungi. Approved standard M38-A; NCCLS 2002; Wayne.

20. Asha A, Imelda J, Paul R.R. Biomass estimation of A. niger S14 a mangrove fungal isolate and A. oryzae NCIM 1212 in solid-state fermentation. J. Mar. Biology. 2006; 48: 139-146.

21. Ng AM, Chan CM, Guo MY, Leung YH, Djurišić AB, Hu X, et al. Antibacterial and photocatalytic activity of TiO2 and ZnO nanomaterials in phosphate buffer and saline solution. Appl Microbiol Biotechnol. 2013; 97: 5565-5573.

22. ELLMAN GL. Tissue sulfhydryl groups. Arch Biochem Biophys. 1959; 82: 70-77.

23. Moghri-Moazzen MA, Borghei SM, Taleshi F. Synthesis and Characterization of Nano-Sized Hexagonal and Spherical Nanoparticles of Zinc Oxide. J. Nano Structure. 2012; 2: 295-300.

24. Khan A. Raman Spectroscopic Study of the ZnO Nanostructures. J Pak Mater Soc. 2010; 4-8.

25. Bai S, Hu J, Li D, Luo R, Chen A, Liu CC. Quantum-sized ZnO nanoparticles: Synthesis, characterization and sensing properties for NO2. J. Mater. Chem. 2011; 21: 12288-12294.

26. Zhang YB, Ali SF, Dervishi E, Xu Y, Li ZR, Casciano D, et al. Cytotoxicity effects of graphene and single-wall carbon nanotubes in neural phaeochromocytoma-derived PC12 cells. ACS Nano. 2010; 4: 3181-3186.

27. Zhang H, Shan Y, Dong L. A comparison of TiO2 and ZnO nanoparticles as photosensitizers in photodynamic therapy for cancer. J Biomed Nanotechnol. 2014; 10: 1450-1457.

28. Devashri S, Kannan GM, Vijayaraghavan R, Anand T, Farhath K. Nanosized Zinc Oxide Induces Toxicity in Human Lung Cells. ISRN Toxicology. 2013; 316075.

29. Fahey RC, Brown WC, Adams WB, Worsham MB. Occurrence of Glutathione in Bacteria. J. Bacteriol., 1978; 133: 1126-1132.

Cite this article

Navale GR, Thripuranthaka M, Late DJ, Shinde SS (2015) Antimicrobial Activity of ZnO Nanoparticles against Pathogenic Bacteria and Fungi. JSM Nanotechnol Nanomed 3(1): 1033.